

Accepted Manuscript

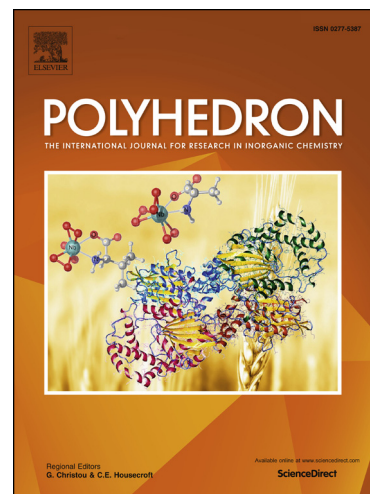
Structural insights into the usage of carboxylate ions as molecular pins

Marcin Swiatkowski, Rafal Kruszynski

PII: S0277-5387(17)30494-1
DOI: <http://dx.doi.org/10.1016/j.poly.2017.07.011>
Reference: POLY 12747

To appear in: *Polyhedron*

Received Date: 4 April 2017
Revised Date: 15 July 2017
Accepted Date: 17 July 2017



Please cite this article as: M. Swiatkowski, R. Kruszynski, Structural insights into the usage of carboxylate ions as molecular pins, *Polyhedron* (2017), doi: <http://dx.doi.org/10.1016/j.poly.2017.07.011>

This is a PDF file of an unedited manuscript that has been accepted for publication. As a service to our customers we are providing this early version of the manuscript. The manuscript will undergo copyediting, typesetting, and review of the resulting proof before it is published in its final form. Please note that during the production process errors may be discovered which could affect the content, and all legal disclaimers that apply to the journal pertain.

Structural insights into the usage of carboxylate ions as molecular pins

Marcin Swiatkowski, Rafal Kruszynski

*Institute of General and Ecological Chemistry
Lodz University of Technology, Zeromskiego 116, 90-924, Lodz, Poland*

Abstract

Two series of new isostructural coordination compounds containing cobalt, nickel, copper butyrates (butyr) or isobutyrate (ibutyr) and 1,10-phenanthroline (phen), of general formulas $[M(phen)_3]^{2+} \cdot 2(butyr) \cdot 11H_2O$ and $[M(phen)_3]^{2+} \cdot 2(ibutyr) \cdot 14H_2O$, were synthesized in water solutions and characterized by X-ray crystallography, IR, UV-Vis and fluorescence spectroscopy, elemental and thermal analysis. The carboxylate anions are located in an outer coordination sphere, which is a unique phenomenon in case of ibutyr coordination compounds. The studied compounds exhibit layered packing in crystal net. The “aqueous layers” consist of water molecules and carboxylate groups of carboxylate anions, assembled *via* hydrogen bonds to the two dimensional supramolecular networks containing multiple different cyclic motifs. Coordination units together with aliphatic ends of carboxylate anions form the “coordination moieties layers”, which are internally connected *via* $\pi \cdots \pi$ and $C-H \cdots \pi$ intermolecular interactions. The carboxylate anions function as supramolecular linkers between these layers and allow pinning them together. The spectroscopic and thermal properties have been discussed and correlated with molecular structures of the studied compounds. Due to placement of carboxylate anions out of coordination moieties, the presented compounds can be ideal standards in spectroscopic determinations of coordination type of butyr and ibutyr ions in coordination compounds. The thermal analyses of the studied compounds revealed the possibility of formation of dihydrate forms, and such dihydrated compounds cannot be produced in direct synthesis performed in aqueous media. In properly set environment the studied compounds can be thermally converted to micro- and nanoparticles of respective metal oxides.

Keywords: 1,10-phenanthroline; cobalt; nickel; copper; nanoparticles

1. Introduction

Nowadays, coordination chemistry is one of the most important field of chemistry. It gives endless possibilities to create metal and semimetal coordination compounds with organic and inorganic molecules [1, 2, 3, 4, 5, 6, 7, 8, 9, 10, 11, 12]. Structural investigations allow determination of correlation between the structure of compounds and their physicochemical properties. Such relationships are the basis of intentional application of coordination compounds in practice [13, 14, 15]. In property-designed synthesis, the most popular are N-donor ligands. These ligands are often utilized solely (or with O-donor ligands) in construction of structurally variable coordination compounds. 1,10-Phenanthroline (phen) is a model representative of this group of ligands. It possesses two close deshielded nitrogen atoms, thus it is a perfect bidentate chelating ligand [16, 17, 18]. The phen typically acts as a bidentate ligand. Few compounds with chelating-bridging phen were synthesised, but this coordination mode is extremely rare [19]. The most popular metal : phen stoichiometry in an inner coordination sphere of mononuclear coordination compounds is 1:1 (2157 compounds structures deposited in

Cambridge Structural Databases [20]), slightly less popular stoichiometry is 1:2 (1299 compounds structures), and next are the stoichiometries: 1:3 (563 compounds structures), 1:4 (9 compounds structures), and 1:5 (1 compound structure) [21].

Phen is employed willingly in many fields of science and industry. It is commonly used in analytical chemistry as an indicator in quantitative determination of metal cations (e.g. in spectrophotometric determination of iron(II) [22]). Some coordination compounds with metal : phen stoichiometry 1:1, like $[\text{MgSO}_4(\text{H}_2\text{O})_3(\text{phen})]$ and $[\text{ZnBr}_2(\text{phen})]$, are efficient luminescent materials [23, 24]. These compounds absorb radiation from UV region and exhibit strong blue or green fluorescence, thus can be employed as perfect UV sensors. Recently, compounds with phen have been widely studied in terms of DNA interactions and cytotoxicity [25]. Coordination compounds of copper(II) with phen and other ligands possess anti-proliferative activity against cancer [26]. Due to catalytic activity toward reactive oxygen species, such compounds are able to induce breakage of DNA strands in aqueous solution without presence of any external reducing factors. Palladium(II) compounds with phen are cytotoxic against chronic *myelogenous leukemia* cells [27] while rhodium(III) and iridium(III) mononuclear compounds with phen derivatives exhibit anti-proliferative activity toward *Jurkat leukemia* cells [28]. There is also possible to reduce, or even completely inhibit, a growth of many cell lines of bacteria and fungi with usage of phen coordination compounds. The $[\text{Cu}(\text{SAla})\text{phen}]\cdot\text{H}_2\text{O}$ (SAla – salicylidenealanine) manifests strong antibacterial activity against i.a. *Salmonella typhi*, and antifungal activity against i.a. *Candida albicans* [29]. Coordination compounds of phen and phen derivatives can be used effectively as substrates in the single precursor method for production of metal oxide nanoparticles [30, 31, 32].

The current work deals with the synthesis, structure, spectroscopic and thermal properties of six new coordination compounds of cobalt, nickel and copper butyrates/isobutyrate with phen (of which compounds with the same anions are isostructural), of general formulae $[\text{M}(\text{phen})_3]^{2+}\cdot 2(\text{butyr})\cdot 11\text{H}_2\text{O}$ and $[\text{M}(\text{phen})_3]^{2+}\cdot 2(\text{ibutyr})\cdot 14\text{H}_2\text{O}$ ($\text{M} = \text{Co}, \text{Ni}, \text{Cu}$, respectively for compounds **1**, **2**, **3** containing butyr anion and for compounds **4**, **5**, **6** containing ibutyr anion), possessing less typical 1:3 metal : phen stoichiometry. The possibility of conversion of compounds **1-6** into nanoparticles (*via* single precursor method) is also presented and discussed. The butyr and ibutyr anions are long enough for possessing well separate hydrophobic properties (at the aliphatic end) and hydrophilic properties (at the carboxylate end), and thus they can be used for assembling of the supramolecular layers constructed from purely hydrophobic ($\text{M}(\text{phen})_3$ in studied case) and hydrophilic (H_2O) moieties.

2. Experimental

2.1. Synthesis

All reagents were analytical grade. Butyric acid (butyrH) and isobutyric acid (ibutyrH) were obtained from Sigma-Aldrich, and all other chemicals were purchased from POCh S.A. The analytical grade water was obtained from improved drinking water *via* combined reverse osmosis and ion exchange processes.

2.1.1. Preparation of butyrate and isobutyrate salts

The aqueous solutions of $\text{Co}(\text{butyr})_2$, $\text{Ni}(\text{butyr})_2$, $\text{Cu}(\text{butyr})_2$, $\text{Co}(\text{ibutyr})_2$, $\text{Ni}(\text{ibutyr})_2$ and $\text{Cu}(\text{ibutyr})_2$ were synthesized in reaction between appropriate metal oxide and butyrH or ibutyrH. 4.2 mmol of each metal oxide was suspended in 100 cm³ of water, and then 8 mmol of 99% butyrH (0.74 cm³, $d = 0.958 \text{ g/cm}^3$ in 25°C) or 99% ibutyrH (0.75 cm³, $d = 0.95 \text{ g/cm}^3$ in 25°C) was added. Such 6 mixtures (each metal oxide with each acid) were being heated at 100°C under reflux for 3h. Next, the suspensions were filtered in order to remove

excess of metal oxide. The concentrations of Co^{2+} , Ni^{2+} and Cu^{2+} in resulting filtrates were determined *via* edta titration in presence of pyrogallol red, pyrocatechol violet and 1-(2-pyridylazo)-2-naphtol, respectively for the above mentioned cations [33].

2.1.2. Preparation of coordination compounds

The coordination compounds **1-6** were prepared by reaction of appropriate butyrate or isobutyrate salts with 1,10-phenanthroline in molar stoichiometry of reagents 1:3. 3 mmol of phen were dissolved in mixture of methanol and water ($5 + 5 \text{ cm}^3$) and added dropwise to every above described water solutions containing 1 mmol of appropriate salt. The reaction mixtures were being stirred vigorously at room temperature for 20 minutes. The solutions were left to crystallize. After one month, the grown colour crystals (brown – cobalt compounds, burgundy – nickel compounds, blue – copper compounds) were filtered off and dried in air.

2.1.3. Preparation of micro- and nanoparticles of metal oxides

The coordination precursors **1-6** were converted to micro- and nanoparticles of respective metal oxides *via* controlled thermal decomposition (carried out in corundum crucibles placed in a muffle furnace, in air atmosphere). Two experiments were performed. In the first one (E1), samples of **1-6** were heated with heating rate $5 \text{ }^\circ\text{C min}^{-1}$ to temperature of formation of respective metal oxide (determined individually for each coordination compound, on the basis of thermal analyses, i.e. 500, 500, 520, 490, 490 and 550 $^\circ\text{C}$ respectively for **1-6**). In the second one (E2), samples were placed in a furnace initially heated to the determined temperature of formation of respective metal oxide.

2.2. Crystal structure determination

Crystals were mounted in turn on the KM-4-CCD automatic diffractometer equipped with the CCD detector, and used for data collection. X-ray intensity data were collected with graphite-monochromated $\text{CuK}\alpha_1$ radiation ($\lambda = 1.54178 \text{ \AA}$) at 100.0(1) K, with ω scan mode. Lorentz, polarization, decay and numerical absorption corrections were applied [34]. The structures were solved by partial structure expansion procedure. All non-hydrogen atoms were refined anisotropically using full-matrix, least-squares method on F^2 . All hydrogen atoms were found on the difference Fourier syntheses and were refined in riding model. Isotropic displacement factors of hydrogen atoms were equal to 1.2 and 1.5 times a value of equivalent displacement factor of parent carbon and oxygen atoms, respectively. Carbon-bonded hydrogen atom positions were idealized after each cycle of refinement. The SHELXT [35], SHELXL [36], and SHELXTL [37] programs were used for all calculations. Atomic scattering factors were those incorporated in the computer programs. The details concerning crystal data, refinement and selected structural data of compounds **1-6** are given in Tables 1-4. One of butyr anions in compound **2** is disordered over two positions with 0.59 : 0.41 participation of domains. It affects the number of water molecules located in the crystal net of compound **2** (in comparison to compound **1** and **3**), because water molecules share the positions of the crystal net with the minor disordered domain of butyr anion. Some displacement ellipsoids of outer coordination sphere species exhibit prolation or oblation effects, probably as a result of disorder. Introduction of disorder models (containing two or three domains) leads to worsening of refinement parameters as well some instability of refinement. Consequently, it can be assume that the disorder is dynamical in character or is a multipositional one, and thus these models were not applied in the final refinement. In case of compounds **1** and **3**, above mentioned effects lead to worse quality of structure determination, but this fact did not affect the unambiguity of the structural determinations themselves. The further details on the structures refinement are given in the supplementary materials (paragraph S2.2).

2.3. Other measurements

The IR spectra of the studied compounds were recorded on the Jasco FT/IR 6200 spectrophotometer, in the spectral range 4000 – 400 cm^{-1} , as KBr pellets. The UV-Vis diffuse reflectance spectra were recorded on the Jasco V-660 spectrophotometer, in spectral range 200 – 800 nm, using BaSO_4 as a standard with 100% reflectance. The three dimensional fluorescence spectra were recorded on the Jasco FP-6300 spectrofluorometer, with solid samples directed at the angle of 30° to incident beam. Data pitch and bandwidth were 1 nm on both monochromators. The thermal analyses were carried out in the TG/DTA (SETSYS-16/18) thermoanalyser coupled with the mass spectrometer (QMS-422; ThermoStar Balzers Instruments). The samples were heated in corundum crucibles up to 1000 $^\circ\text{C}$ at a heating rate of $5^\circ\text{C}\cdot\text{min}^{-1}$ in air flow. The final products of decomposition were confirmed by X-ray powder diffraction (XRPD) using the Powder Diffraction File [38] or literature data. The XRPD patterns were measured in reflection mode on the XPert PRO X-ray powder diffraction system, equipped with the Bragg-Brentano PW 3050/65 high resolution goniometer and the PW 3011/20 proportional point detector. The $\text{CuK}\alpha_1$ radiation was used. The patterns were measured at 291.0(2) K in range $2 - 90^\circ$ with the narrowest beam attenuator. Diamond powder was used as an internal reference. The surface morphologies of micro- and nanoparticles of metal oxides were characterized by the scanning electron microscope with energy dispersive X-ray spectrometer (SEM-EDS, HITACHI S-4700, EDS Thermo NORAN). Elemental analyses were carried out using the Vario EL III CHNOS Elemental Analyzer (C, H, N, O). Cobalt(II), nickel(II) and copper(II) contents were determined by titration with edta, as described in paragraph 2.1.1. [33]. Elemental analyses for coordination compounds [Calc./Found (%)]:

(1) $\text{C}_{44}\text{H}_{60}\text{CoN}_6\text{O}_{15}$ C 54.36/54.10; H 6.23/6.51; Co 6.06/5.92; N 8.65/8.78; O 24.69/24.82; (2) $\text{C}_{44}\text{H}_{58.35}\text{Ni}_6\text{NiO}_{14.18}$ C 55.23/54.89; H 6.15/6.49; N 8.78/8.44; Ni 6.13/5.78; O 23.71/24.73; (3) $\text{C}_{44}\text{H}_{60}\text{CuN}_6\text{O}_{15}$ C 54.11/54.02; H 6.20/6.31; Cu 6.51/6.20; N 8.61/8.74; O 24.57/24.60; (4) $\text{C}_{44}\text{H}_{66}\text{CoN}_6\text{O}_{18}$ C 51.50/51.59; H 6.50/6.45; Co 5.74/5.51; N 8.19/8.28; O 28.07/28.14; (5) $\text{C}_{44}\text{H}_{66}\text{Ni}_6\text{NiO}_{18}$ C 51.51/51.57; H 6.50/6.41; N 8.19/8.24; Ni 5.72/5.49; O 28.07/28.21; (6) $\text{C}_{44}\text{H}_{66}\text{CuN}_6\text{O}_{18}$ C 51.27/51.21; H 6.47/6.59; Cu 6.17/5.97; N 8.16/8.10; O 27.94/27.90.

3. Results and discussion

The reactions of butyr and ibutyr salts with phen lead to formation of two isostructural series of compounds, with general formulae: $[\text{M}(\text{phen})_3]^{2+}\cdot 2(\text{butyr})\cdot 11\text{H}_2\text{O}$ and $[\text{M}(\text{phen})_3]^{2+}\cdot 2(\text{ibutyr})\cdot 14\text{H}_2\text{O}$ (Fig. 1). The isostructurality among coordination compounds is observed due to i.a. replacement of a metal cation for another one, with close ionic radius. It is possible for the presented coordination compounds, since the ionic radii of cobalt(II), nickel(II) and copper(II) are very similar (0.74, 0.69 and 0.73 Å, respectively [39]). The applied in the synthesis 1:3 metal : ligand stoichiometry is retained in the crystal structures of obtained compounds. The inner coordination spheres of discussed compounds are created by a central atom and three bidentate chelating molecules of phen. In each case, the coordination polyhedron is slightly distorted octahedron [40] (Table 2). A weak compressive Jahn-Teller effect observed in the copper compounds causes that distortions in them are slightly larger than in the cobalt and nickel compounds. The central atoms of ibutyr coordination compounds are located at the special position e of the $\text{C}2/c$ space group (with site symmetry 2 and multiplicity 4), whereas all atoms of butyr coordination compounds occupy the general positions. Despite that, the coordination units of both compounds groups are quite similar (Fig. S2). Therefore, the existence of compounds in different space groups

(*P*-1 and *C*2/*c*) is not a consequence of differences in phen positions around the central atom. This difference results from the existence of the different isomer of anion. The structural differences between anions cause presence of different number of water molecules in the outer coordination sphere (even and odd) and subsequently lead to their less symmetrical location in the butyr compounds.

The correctness of assignment of the central atoms formal oxidation states was confirmed with usage of the bond-valence method. The bond valences were computed as $\nu_{ij} = \exp[(R_{ij}-d_{ij})/b]$ [41, 42], where R_{ij} is the bond-valence parameter (in the formal sense R_{ij} can be considered as a parameter equals to the idealized single-bond length between *i* and *j* atoms for given *b*) and *b* was taken as 0.37 Å [43, 44]. The R_{Co-N} , R_{Ni-N} , and R_{Cu-N} were re-determined for coordination compounds, as it was previously described [45, 46, 47], and their values were 1.727, 1.674 and 1.752, respectively. The computed bond valences are collected in Table 2. The computed total valences of central atoms (BVS) are very close to the expected value of +2 (formal oxidation state of metal), and in each case, a deviation of BVS is smaller than value of 0.25 - 0.30 v.u. [48], which exceeding could indicate mistakes in an interpretation of the compound structure or in a charge of an ion. The largest deviations are noted for the copper coordination compounds (2.174 and 2.181 v.u. respectively for **3** and **6**), due to a weak compressive Jahn-Teller effect. Two of three chelating molecules of phen coordinate stronger by one of two nitrogen-donor atoms (phen ligands coordinate asymmetrically to the central atom), as a result of rigid restrains imposed by stiff chelating ligand. Consequently, one coordination bond has expected strength, but second of them is significantly stronger (by about 0.1 v.u.), what causes positive deviation of BVS.

All butyr and ibutyr ions are located in the outer coordination sphere. It is a unique phenomenon for ibutyr, not structurally proved in literature, because in coordination compounds (with determined crystal structures) ibutyr always acts as a ligand directly coordinating a metal ion. For butyr, there are only three compounds reported in Cambridge Structural Database [20], in which this anion is placed out of coordination moieties, i.e. *catena*(tetra-aqua-(μ_2 -butyrato)-magnesium butyrate) [49], (μ_2 -butanoato-O,O')-monoqua-ethanolato-bis(1,2-bis(salicylaldiminato)ethane)-di-manganese butyrate [50], heptatriaconta-ammonium tetracosakis(butyrate) molybdate hydrate [51]. Apart from carboxylate anions, there are 11 and 14 water molecules in the outer coordination sphere, respectively for butyr and ibutyr coordination compounds. As a consequence of different properties of species forming the compounds (coordination moieties, anions and water molecules), two layers are created in the crystal nets: the “aqueous layer” and the “coordination moieties layer”, containing respective species (Fig. 2). Due to the content, the layers can be considered as hydrophilic (rich in O-H hydrogen bond donors and O hydrogen bond acceptors) and hydrophobic (rich in π electrons and C-H groups). The carboxylate anions connect these layers, because the carboxylate groups take part in formation of hydrogen bonds with water molecules (hydrophilic end of anion) and the aliphatic groups are located in the “coordination moieties layer” (hydrophobic end of anion). The water molecules and carboxylate anions are assembled to the two dimensional supramolecular networks *via* hydrogen bonds (Table 3). These bonds form different multiple cyclic motifs, characterized by: $N_2R_4^2(8)$, $N_3R_3^3(8)$, $N_3R_6^6(12)$, $N_3R_6^6(16)$, $N_4R_4^3(8)$, $N_4R_8^6(16)$, $N_5R_5^3(10)$, $N_5R_5^5(12)$, $N_6R_6^4(12)$, $N_6R_6^5(12)$ graphs for butyr compounds (respectively 1-10 in Fig. 3a), and $N_2R_4^4(8)$, $N_3R_3^3(8)$, $N_3R_6^6(12)$, $N_5R_5^4(10)$, $N_5R_5^4(12)$ for ibutyr compounds (respectively 1-5 in Fig. 3b). According to classification of the extended water motifs [52], these existing in the studied compounds can be classified as the infinite layer motifs in two dimensions and can be described as L4(5)4(6)5(5)5(6)6(6)6(7)7(9)8(12)10(10) and L4(6)5(6)5(7)6(8)7(8), respectively for butyr and ibutyr compounds. Noteworthy is the fact that, such motifs

have been not registered for any structurally characterized compound, and they can be expressed as the six petals flower-like motifs (Fig. 3).

The “coordination moieties layer” is stabilized in both compounds groups *via* $\pi\cdots\pi$ and $C-H\cdots\pi$ intermolecular interactions (Table 4). In the butyr compounds, only one phen ligand of the coordination unit takes part in $\pi\cdots\pi$ stacking interactions. This phen molecule associates with the alternatively orientated equivalent phen molecule by two of three delocalized rings (stacking type XII [53], Fig. S7a). The formed $\pi\cdots\pi$ supramolecular dimers of the coordination units interact indirectly with other ones through the butyr anions. Each carboxylate ion, located between two phen molecules of two coordination entities, associates with them by $C-H\cdots\pi$ interactions (Fig. S7a). In consequence, the two dimensional supramolecular net is formed. The intermolecular interactions array is significantly different for the ibutyr compounds. The $\pi\cdots\pi$ interactions are formed by two phen molecules of each coordination unit. Only carbon (C_6) rings take part in association (stacking type XIII, Fig. S7b). Therefore, the coordination entities are assembled to the parallel one dimensional chains, extending along crystallographic [001] axis. The ibutyr anions, in opposition to the butyr ones, do not act as supramolecular linkers between the coordination entities. Each ibutyr anion associates *via* $C-H\cdots\pi$ interactions with only one phen molecule (Fig. S7b).

The isostructurality resulting from replacement of a metal cation causes that the IR spectra of studied butyr as well as ibutyr coordination compounds are almost perfectly identical within each group, in investigated range of wavenumbers (Table 5, Fig. S3). The large number of water molecules in crystal structures of both compounds groups is visible in the IR spectra of these compounds as two typical bands originating from OH stretching and bending vibrations. They fall over 3100 cm^{-1} (strongly broadened band as a result of different environment of each water molecule and consequently different energies of specific oscillators) and about 1650 cm^{-1} , respectively. In comparison to the spectrum of pure phen, the typical for chelating molecules blue shifts of bands corresponding to CC and CN stretching vibrations are observed [23, 24, 53]. The spectra of the studied compounds exhibit also a set of bands characteristic for aliphatic parts of carboxylate anions, including stretching and various bending vibrations of CH and CC bonds. The asymmetric (ν_{as}) and symmetric (ν_s) stretching vibrations of carboxylate groups reflect in strong bands at about 1550 (cobalt and nickel compounds) and 1560 (copper compounds) for the former ones, and 1425 cm^{-1} (all compounds) for the latter ones. The location of carboxylate anions in outer coordination sphere results in shift of the ν_{as} bands toward lower frequencies (in comparison to pure salts). The carboxylate group participates only in hydrogen bonds with water molecules, therefore it possesses larger oscillation freedom (the energy required to excite vibrations is lower in comparison to pure salts, in which carboxylate anions coordinate directly to central atoms) [54]. Due to such location of carboxylate anions, the studied compounds can be ideal standards in spectroscopic determinations of coordination type of butyr and ibutyr ions in coordination compounds. This can be achieved with usage of the $\Delta\nu$ parameter, i.e. the difference between wavenumbers of ν_{as} and ν_s of carboxylate group. The $\Delta\nu$ parameter is commonly used to distinguish a functionality and a denticity of carboxylate groups, but for correct usage a reference compounds with unambiguously determined structure (*via* other method) must be known [55, 56]. It must be outlined that, although the $\Delta\nu$ is the same for cobalt and nickel compounds (127 and 126 cm^{-1} , respectively for butyr and ibutyr compounds), it is different for copper compounds (138 and 135 cm^{-1} , as above). This indicates that the comparison of the $\Delta\nu$ values must also cover a consideration of central atoms and should not be limited to a consideration of sole carboxylate anion. The determined values are distinctly different than

values calculated for butyr and ibutyr anions acting as bidentate chelating ligands, e.g. $\Delta\nu$ values for (butanoato)-bis(N-(pyridin-2-yl)pyridin-2-amine)-cobalt(II) chloride [57], (butanoato)-bis(N-(pyridin-2-yl)pyridin-2-amine)-nickel(II) chloride [57], (2-methylpropanoato)-bis(1,10-phenanthroline)-copper(II) nitrate dihydrate [58], are 164, 166, and 167 cm^{-1} , respectively. The $\Delta\nu$ values for butyr and ibutyr located in an inner coordination sphere are larger than $\Delta\nu$ values determined for these anions located in an outer coordination sphere by about 30-40 cm^{-1} . Such difference is large enough for determination of ligand location in an outer coordination sphere on the basis of IR data. It also proves a usefulness of the studied compounds in establishing of coordination type of butyr and ibutyr ions *via* IR spectroscopy.

The solid state UV-Vis spectra of the studied compounds contain several absorption maxima (Table 6, Fig. S4). In investigated wavelength range, solid state phen exhibits five absorption maxima at 214, 253, 294, 324, 335 nm corresponding to $\pi \rightarrow \pi^*$ (first two maxima) and $n \rightarrow \pi^*$ (last three maxima) transitions [24], which are also present in the spectra of **1-6**. Generally, these maxima are red-shifted in all cases, due to stronger $\pi \cdots \pi$ stacking interactions in pure phen (than in coordination compounds) in case of $\pi \rightarrow \pi^*$ transitions [23], and due to participation of nitrogen lone electron pairs of phen in coordination bonds, what leads to decrease the energy as well as the population of $n \rightarrow \pi^*$ transitions [24]. The intense colour of the studied compounds originates from $d-d$ transitions. Due to analogous distorted octahedral geometry of coordination polyhedra, the same maxima are observed in the spectra of compounds of the same cation. Three transitions are expected for both cobalt [$^4T_{1g}(F) \rightarrow ^4T_{2g}(P)$ (ν_1), $^4T_{1g}(F) \rightarrow ^4A_{2g}(F)$ (ν_2), $^4T_{1g}(F) \rightarrow ^4T_{1g}(P)$ (ν_3)] and nickel compounds [$^3A_{2g} \rightarrow ^3T_{2g}(F)$ (ν_1), $^3A_{2g} \rightarrow ^3T_{1g}(F)$ (ν_2), $^3A_{2g} \rightarrow ^3T_{1g}(P)$ (ν_3)] [59]. The registered spectra of cobalt compounds contain solely maximum corresponding to the highest energy $d-d$ transition (ν_3). The second one (ν_2), which is forbidden two-electron transition and is usually observed as a weak shoulder maximum [60], is not present in the spectra of the studied compounds. The lowest energy transition (ν_1) exists in near-IR region (1078 nm [61], 1248, 1256 nm [62]), so it is out of investigated range. In case of nickel compounds, the ν_3 and ν_2 transitions are observed as two maxima in visible and slightly above visible region, respectively. Similarly to cobalt compounds, the ν_1 transition is also outside of the measurement region (985 nm [63], 967 nm [61], 998, 1086, 1135, 1256 nm [62]). Blue colour of copper compounds is due to the broad absorption maximum at about 680 nm. The $^2E_g \rightarrow ^2T_{2g}(F)$ transition is expected in octahedral copper compounds, but due to weak compressive Jahn-Teller effect in **3** and **6**, it splits into three transitions $^2B_{1g} \rightarrow ^2A_{1g}$ (ν_1), $^2B_{1g} \rightarrow ^2B_{2g}$ (ν_2), $^2B_{1g} \rightarrow ^2E_g$ (ν_3). All these e transitions are closely similar in energy, therefore they exist in studied spectra as single broad maximum [64, 65]. The maxima in 400 – 460 nm range originates from ligand – metal charge transfer transitions (LMCTs). The LMCTs are not observed in copper compounds, what was previously reported for $[\text{Cu}(\text{phen})_3]^{2+}$ compounds [66, 67, 68].

The fluorescence properties of pure phen make it suitable for constructing of fluorescent materials. The pure phen exhibits three emission maxima at 363, 381 and 431 nm for 341, 345 and 371 nm excitation wavelengths, respectively (Fig. S5a) [24]. The studied compounds do not possess even weak fluorescence properties in solid state (Fig. S5b) as a result of vibrational relaxation blockage of excited state by the stiff, strongly restrained and sterically hindered $[\text{M}(\text{phen})_3]^{2+}$ system.

The thermal analyses of **1-6** revealed the same decomposition pathway for all compounds, what can be expected due to analogous structures of butyr and ibutyr compounds (Table 7, Fig. S6, Scheme S1). As a result of large number of water molecules in an outer coordination sphere, the studied compounds are not very stable and start to decompose at 30-40°C. The first stage of decomposition is the endothermic dehydration during

which 9 and 12 water molecules (respectively for butyr and ibutyr compounds) are evaporated, what causes that two water molecules remain in structure of each compound. It means that all studied compounds can also exist as dihydrates, but the obtainment of such dihydrate form is impossible *via* standard crystallization. The IR spectra of these dihydrates suggest that remaining water molecules are bonded to carboxylate anions *via* O-H...O hydrogen bonds. The dihydrates are stable up to 175-185 °C, and then the second decomposition stage begins. This stage is a combination of simultaneous removal of remaining two water molecules and combustion of carboxylate anions. The strong exothermic process of phen decomposition starts at about 360-400 °C, but only in case of **1**, **4** and **6**, it is possible to distinguish the border between the second and the third decomposition stage. For the rest compounds, these two stages are slightly overlapped. In all cases, the final decomposition product is the respective metal oxide, stable to the highest measured temperature (1000°C).

The controlled thermal conversion of coordination precursors **1-6** leads to formation of bulky or porous particles (of micro and nano size, Fig. 4 and 5) of cubic NiO/CoO (rock salt structure, $a = b = c = 4.178 \text{ \AA}$ (for NiO) and 4.263 \AA (for CoO), $Z = 4$, space group $Fm-3m$, No. 225) and of monoclinic CuO ($a = 4.684 \text{ \AA}$, $b = 3.423 \text{ \AA}$, $c = 5.129 \text{ \AA}$, $\beta = 99.54(1)^\circ$, $Z = 4$, space group $C2/c$, No. 15). The formed particles exhibited significant differences in morphology and/or size. These differences originate from three factors: structure of precursors, structure of products and thermal conversion parameters. The cubic oxides form large plates and prisms composed of small agglomerated spherical nanoparticles. These agglomerates contain nano-sized crack and pores. The pores are better shaped and more regular in case of oxides produced from compounds containing butyr ions, as a result of deeper penetration of the “coordination moieties layer” by these ions and stronger “inflating” of the particles during decomposition. The same phenomenon is responsible for formation of larger pores upon instant heating of sample (experiment E2, paragraph 2.1.3.). The monoclinic oxide exists in form of nanospheres agglomerated into complex 3D architectures. The instant heating of sample (E2) leads to larger agglomeration than observed for slow heating (experiment E1, paragraph 2.1.3.). The E2 nanoparticles form smooth microstructures, whereas the E1 nanoparticles are assembled into protruding micrograins. Similarly to cubic oxides and due to the same reasons, the monoclinic oxide created from the compound containing butyr ions is dispersed at larger degree than observed for oxide based on ibutyr compounds. Combination of slow heating (E1) and structure of precursor based on an ibutyr ion allows formation of raspberry-like microentities (Fig. 5(6_CuO_E1) and Fig. S8).

4. Conclusions

1,10-Phenanthroline with cobalt, nickel, copper butyrates and isobutyrate forms two groups of isostructural coordination compounds (of general formulas $[M(\text{phen})_3]^{2+} \cdot 2(\text{butyr}) \cdot 11\text{H}_2\text{O}$ and $[M(\text{phen})_3]^{2+} \cdot 2(\text{ibutyr}) \cdot 14\text{H}_2\text{O}$), as a result of direct reactions between mentioned species in an aqueous medium. The existence of a different isomer of the anion and consequently different number of water molecules in an outer coordination sphere subsequently leads to less symmetrical location of them in butyr compounds and forces adoption of different space groups ($P-1$ and $C2/c$, respectively for butyr and ibutyr compounds). The layered crystal structures of studied compounds are stabilized *via* hydrogen bonds network in the “aqueous layer” (hydrophilic one), and *via* $\pi \cdots \pi$ interactions in the “coordination moieties layer” (hydrophobic one). Additional connection between layers is provided by carboxylate anions, which interact with both layers *via* hydrogen bonds and C—H... π interactions, respectively. Consequently, carboxylate anions function as

supramolecular linkers between these layers and allow pinning them together. The studied compounds can be ideal standards in spectroscopic determination of a coordination type of butyr and ibutyr in coordination compounds, due to location of such carboxylates in an outer coordination sphere. The determined $\Delta\nu$ parameter for non-coordinating butyr and ibutyr anions is about 127 cm^{-1} for cobalt and nickel compounds, and 137 cm^{-1} for copper compounds. The IR and UV-Vis spectra contain bands and maxima expected for chelating phen molecules. The octahedral geometries of coordination polyhedra result in appropriate maxima in visible region. A weak compressive Jahn-Teller effect causes considerable spectral changes in the Vis region of UV-Vis spectra of copper compounds. The thermal analyses of **1-6** reveal existence of a dihydrate form of each of them, which is impossible to obtain in direct synthesis in aqueous media. The compounds **1-6** can be converted to metal oxide micro and nanoparticles with usage of single precursor method, and the topology and size of formed particles is governed by structure of precursors, structure of products and thermal conversion parameters.

Appendix A. Supplementary data

CCDC 1542008, 1542009, 1542010, 1425088, 1425087 and 1425089 contain the supplementary crystallographic data for **1-6**. These data can be obtained free of charge via <http://www.ccdc.cam.ac.uk/conts/retrieving.html>, or from the Cambridge Crystallographic Data Centre, 12 Union Road, Cambridge CB2 1EZ, UK; fax: (+44) 1223-336-033; or e-mail: deposit@ccdc.cam.ac.uk.

Acknowledgments

This work part was financed by funds allocated by the Ministry of Science and Higher Education to the Institute of General and Ecological Chemistry, Lodz University of Technology.

Figure 1. The solid state structures of compound **2** (a) and compound **5** (b), with atom numbering scheme, plotted with 50% probability of displacement ellipsoids of non-hydrogen atoms. The disordered butyrate of compound **2** ion is indicated by dashed lines. Hydrogen atoms were omitted for clarity. The symmetry generated atoms of compound **5**, indicated by dashed lines and A letter, were generated via $-x, y, -z+0.5$ symmetry transformations.

Figure 2. The part of molecular packing, representing the layered structure of crystal nets of studied compounds. Hydrogen atoms were omitted for clarity.

Figure 3. The multiple cyclic motifs of hydrogen bonds in the “aqueous layers” of butyrate (a) and isobutyrate (b) compounds (aliphatic ends of carboxylate ions were omitted for clarity), and graphic representation of formed six petals flower-like motifs. Letters a, b and c, added to the same number of the cyclic motif, indicate the same graph, but formed by different molecules.

Figure 4. The SEM micrographs of CoO and NiO particles produced from compounds **1, 2, 4** and **5** in two experiments (E1 and E2).

Figure 5. The SEM micrographs of CuO particles produced from compounds **3** and **6** in two experiments (E1 and E2).

Table 1. Crystal data and structure refinement details for the studied compounds.

Compound	1	2	3
Empirical formula	C ₄₄ H ₆₀ CoN ₆ O ₁₅	C ₄₄ H _{58.35} N ₆ NiO _{14.18}	C ₄₄ H ₆₀ CuN ₆ O ₁₅
Formula weight	971.91	956.91	976.52
Crystal system, space group	Triclinic, <i>P</i> -1 (No. 2)	Triclinic, <i>P</i> -1 (No. 2)	Triclinic, <i>P</i> -1 (No. 2)
Temperature [K]	100(2)	100(2)	100(2)
Unit cell dimensions [Å, °]	a = 11.9803(6) b = 13.2913(7) c = 16.7880(8) α = 73.873(3) β = 79.264(3) γ = 64.185(4)	a = 12.0102(2) b = 13.1672(3) c = 16.7724(3) α = 74.1140(10) β = 78.9010(10) γ = 63.7960(10)	a = 12.0128(12) b = 13.2449(15) c = 16.7821(17) α = 74.484(10) β = 78.848(8) γ = 63.987(9)
Volume [Å ³]	2305.1(2)	2281.02(8)	2303.3(5)
Z, Calculated density [Mg/m ³]	2, 1.400	2, 1.393	2, 1.408
Absorption coefficient [mm ⁻¹]	3.557	1.237	1.308
<i>F</i> (000)	1026	1012	1030
Crystal size [mm]	0.095 x 0.080 x 0.075	0.121 x 0.106 x 0.092	0.121 x 0.108 x 0.095
θ Range for data collection [°]	2.75 to 67.00	3.83 to 67.00	3.80 to 67.00
Index ranges	-13 ≤ <i>h</i> ≤ 11, -15 ≤ <i>k</i> ≤ 15, -19 ≤ <i>l</i> ≤ 20	-14 ≤ <i>h</i> ≤ 14, -15 ≤ <i>k</i> ≤ 13, -20 ≤ <i>l</i> ≤ 20	-14 ≤ <i>h</i> ≤ 12, -15 ≤ <i>k</i> ≤ 15, -20 ≤ <i>l</i> ≤ 20
Reflections collected / unique	23711 / 7903 [<i>R</i> _{int}] = 0.0445]	24351 / 7839 [<i>R</i> _{int}] = 0.0171]	24264 / 7899 [<i>R</i> _{int}] = 0.0200]
Completeness to θ = 25° [%]	96.2	96.4	96.2
Min. and max. transmission	0.740 and 0.778	0.848 and 0.899	0.845 and 0.880
Data / restraints / parameters	7903 / 0 / 598	7839 / 0 / 653	7899 / 0 / 598
Goodness-of-fit on <i>F</i> ²	1.038	1.036	1.993
Final <i>R</i> indices [<i>I</i> > 2 σ (<i>I</i>)]	<i>R</i> 1 = 0.0831, <i>wR</i> 2 = 0.2267	<i>R</i> 1 = 0.0694, <i>wR</i> 2 = 0.1889	<i>R</i> 1 = 0.1057, <i>wR</i> 2 = 0.3716
<i>R</i> indices (all data)	<i>R</i> 1 = 0.0845, <i>wR</i> 2 = 0.2281	<i>R</i> 1 = 0.0713, <i>wR</i> 2 = 0.1904	<i>R</i> 1 = 0.1062, <i>wR</i> 2 = 0.3749
Largest diff. peak and hole [e ⁻ Å ⁻³]	1.656 and -0.903	2.430 and -0.723	2.524 and -1.298

Compound	4	5	6
Empirical formula	C ₄₄ H ₆₆ CoN ₆ O ₁₈	C ₄₄ H ₆₆ N ₆ NiO ₁₈	C ₄₄ H ₆₆ CuN ₆ O ₁₈
Formula weight	1025.95	1025.73	1030.56
Crystal system, space group	Monoclinic, <i>C</i> 2/ <i>c</i> (No. 15)	Monoclinic, <i>C</i> 2/ <i>c</i> (No. 15)	Monoclinic, <i>C</i> 2/ <i>c</i> (No. 15)
Temperature [K]	100(2)	100(2)	100(2)
Unit cell dimensions [Å, °]	a = 22.8520(16) b = 11.8704(9) c = 19.9921(14) α = 90.00 β = 113.545(4) γ = 90.00	a = 22.8571(18) b = 11.8704(10) c = 20.0150(16) α = 90.00 β = 113.421(4) γ = 90.00	a = 22.800(3) b = 11.8973(18) c = 19.967(2) α = 90.00 β = 113.064(9) γ = 90.00
Volume [Å ³]	4971.6(6)	4983.1(7)	4983.3(11)
Z, Calculated density [Mg/m ³]	4, 1.371	4, 1.367	4, 1.374
Absorption coefficient [mm ⁻¹]	3.372	1.226	1.283
<i>F</i> (000)	2172	2176	2180
Crystal size [mm]	0.099 x 0.095 x 0.091	0.105 x 0.093 x 0.090	0.100 x 0.097 x 0.090
θ Range for data collection [°]	4.22 to 72.38	4.22 to 72.57	4.22 to 72.41
Index ranges	-28 ≤ <i>h</i> ≤ 27, -14 ≤ <i>k</i> ≤ 14, -24 ≤ <i>l</i> ≤ 24	-28 ≤ <i>h</i> ≤ 26, -14 ≤ <i>k</i> ≤ 14, -24 ≤ <i>l</i> ≤ 24	-28 ≤ <i>h</i> ≤ 27, -14 ≤ <i>k</i> ≤ 14, -24 ≤ <i>l</i> ≤ 24
Reflections collected / unique	28083 / 4917 [<i>R</i> _{int}] = 0.0233]	27776 / 4936 [<i>R</i> _{int}] = 0.0205]	26811 / 4915 [<i>R</i> _{int}] = 0.0202]
Completeness to θ = 67° [%]	100.0	100.0	99.7
Min. and max. transmission	0.728 and 0.750	0.971 and 0.905	0.868 and 0.906
Data / restraints / parameters	4917 / 0 / 314	4936 / 0 / 315	4915 / 0 / 314
Goodness-of-fit on <i>F</i> ²	1.110	1.046	1.041
Final <i>R</i> indices [<i>I</i> > 2 σ (<i>I</i>)]	<i>R</i> 1 = 0.0641, <i>wR</i> 2 = 0.1727	<i>R</i> 1 = 0.0666, <i>wR</i> 2 = 0.1688	<i>R</i> 1 = 0.0681, <i>wR</i> 2 = 0.1721
<i>R</i> indices (all data)	<i>R</i> 1 = 0.0647, <i>wR</i> 2 = 0.1733	<i>R</i> 1 = 0.0666, <i>wR</i> 2 = 0.1688	<i>R</i> 1 = 0.0682, <i>wR</i> 2 = 0.1723
Largest diff. peak and hole [e ⁻ Å ⁻³]	1.513 and -1.221	1.816 and -1.105	1.683 and -1.280

Table 2. Selected structural data of the studied compounds.

Compound	1	2	3	4	5	6
Symbols	M=Co1	M=Ni1	M=Cu1	M=Co1	M=Ni1	M=Cu1
	N4=N1 ⁱ , N5=N2 ⁱ , N6=N3 ⁱ					
bond length/Å [bond valence/valence units]						
M—N1	2.133(4) [0.334]	2.086(3) [0.328]	2.139(4) [0.351]	2.129(2) [0.337]	2.089(2) [0.326]	2.061(2) [0.434]
M—N2	2.125(4) [0.341]	2.086(3) [0.328]	2.076(3) [0.417]	2.131(2) [0.336]	2.087(2) [0.328]	2.162(2) [0.330]
M—N3	2.113(3) [0.352]	2.079(3) [0.335]	2.145(4) [0.346]	2.129(2) [0.337]	2.088(2) [0.327]	2.166(3) [0.327]
M—N4	2.126(4) [0.338]	2.084(3) [0.330]	2.136(3) [0.354]	2.129(2) [0.337]	2.089(2) [0.326]	2.061(2) [0.434]
M—N5	2.116(3) [0.349]	2.086(3) [0.328]	2.076(3) [0.417]	2.131(2) [0.336]	2.087(2) [0.328]	2.162(2) [0.330]
M—N6	2.152(3) [0.317]	2.105(2) [0.312]	2.211(3) [0.289]	2.129(2) [0.337]	2.088(2) [0.327]	2.166(3) [0.327]
angle/°						
N1—M—N2	78.76(14)	79.92(11)	78.77(13)	78.37(8)	79.91(8)	79.14(9)
N1—M—N3	94.08(13)	93.62(10)	93.43(11)	92.77(8)	92.73(8)	93.12(9)
N1—M—N4	169.03(13)	170.25(10)	168.99(12)	172.16(12)	172.68(12)	171.43(13)
N1—M—N5	92.87(13)	92.54(10)	92.53(12)	95.94(8)	94.82(8)	94.70(9)
N1—M—N6	91.90(12)	91.58(10)	92.66(11)	93.31(8)	92.89(8)	93.56(9)
N2—M—N3	96.72(13)	96.08(10)	97.09(11)	97.22(9)	96.04(8)	97.15(9)
N2—M—N4	93.69(14)	93.13(11)	94.66(12)	95.94(8)	94.82(8)	94.70(9)
N2—M—N5	165.60(13)	167.82(10)	164.77(12)	88.34(12)	89.01(12)	89.09(12)
N2—M—N6	90.35(12)	90.72(10)	89.57(11)	170.47(8)	171.56(8)	170.79(9)
N3—M—N4	78.78(13)	80.24(10)	78.50(12)	93.31(8)	92.88(8)	93.56(9)
N3—M—N5	95.54(13)	93.92(10)	95.88(11)	170.47(8)	171.55(8)	170.79(9)
N3—M—N6	171.51(13)	172.07(11)	171.73(11)	78.37(12)	79.79(12)	77.50(14)
N4—M—N5	96.09(13)	95.41(1)	95.72(11)	78.37(8)	79.91(8)	79.14(9)
N4—M—N6	96.12(13)	95.36(10)	96.14(12)	92.77(8)	92.73(8)	93.12(9)
N5—M—N6	78.13(12)	79.86(9)	78.27(11)	97.22(9)	96.04(8)	97.15(9)

Symmetry transformations used to generate equivalent atoms: (i) -x, y, -z+0.5.

Table 3. Hydrogen bonds in the studied compounds [\AA , $^\circ$].

D-H...A	d(D-H)			d(H...A)			d(D...A)			<(DHA)		
Compound	1	2	3	1	2	3	1	2	3	1	2	3
O89—H89O...O95	0.88	0.88	0.88	1.85	1.90	1.87	2.735(6)	2.776(5)	2.749(7)	179.7	176.3	179.2
O89—H89P...O51	0.89	0.89	0.89	1.92	1.93	1.96	2.812(6)	2.813(5)	2.858(7)	179.6	179.0	179.8
O90—H90O...O51	0.89	0.89	0.89	1.93	2.03	1.97	2.807(6)	2.907(5)	2.845(7)	167.9	168.1	166.7
O90—H91P...O91	0.91	0.91	0.91	2.13	2.24	2.18	3.012(5)	3.112(4)	3.060(7)	164.0	161.6	161.5
O91—H91O...O42 ⁱ	0.91	0.91	0.91	1.99	1.92	2.05	2.902(6)	2.825(6)	2.954(8)	179.6	173.4	175.2
O91—H91P...O52	0.90	0.89	0.90	1.82	1.81	1.78	2.723(5)	2.703(5)	2.681(7)	179.6	177.0	179.0
O92—H92O...O89	0.90	0.90	0.90	1.82	1.83	1.82	2.722(5)	2.729(4)	2.721(5)	179.7	176.4	179.6
O92—H92P...O94	0.91	0.90	0.91	1.87	1.89	1.85	2.780(6)	2.797(5)	2.754(5)	179.8	178.3	178.9
O93—H93O...O98	0.84	0.83	0.83	1.91	1.83	1.86	2.743(6)	2.659(6)	2.690(7)	175.4	174.1	172.7
O93—H93O...O42 ^j		0.83			2.32			3.100(9)			156.1	
O93—H93P...O92	0.88	0.88	0.89	1.91	1.91	1.89	2.786(5)	2.788(4)	2.773(5)	177.1	174.7	175.0
O94—H94O...O93 ⁱⁱ	0.90	0.90	0.90	1.93	1.95	1.99	2.834(6)	2.843(5)	2.885(6)	176.4	175.8	178.5
O94—H94P...O99	0.91	0.90	0.91	2.05	2.04	2.03	2.957(6)	2.942(4)	2.938(6)	176.9	178.7	178.1
O95—H95O...O96	0.90	0.87	0.90	1.77	1.61	1.76	2.674(7)	2.483(7)	2.662(7)	179.6	178.0	177.0
O95—H95O...O41 ^j		0.87			2.36			3.156(10)			151.8	
O95—H95P...O52 ⁱ	0.91	0.90	0.90	1.94	1.94	1.93	2.847(7)	2.841(6)	2.833(7)	179.7	172.9	178.2
O96—H96O...O42	0.88	0.87	0.88	1.79	1.85	1.81	2.661(8)	2.716(8)	2.690(9)	176.9	177.3	175.7
O96—H96P...O98	0.90	0.89	0.88	2.02	2.01	2.05	2.845(6)	2.843(6)	2.845(6)	152.2	154.2	150.5
O97—H97O...O99	0.91	0.91	0.87	1.92	1.96	1.93	2.824(6)	2.858(5)	2.792(7)	170.5	171.6	170.3
O97—H97P...O51	0.89	0.89	0.89	1.92	1.93	1.95	2.804(6)	2.804(5)	2.826(7)	168.1	170.5	168.1
O98—H98O...O41	0.89	0.88	0.88	1.74	1.78	1.70	2.629(7)	2.654(18)	2.586(8)	178.3	178.7	179.0
O98—H98P...O41 ⁱⁱⁱ	0.86	0.86	0.86	1.95	1.94	1.94	2.773(6)	2.767(15)	2.773(6)	159.3	162.5	162.9
O99—H99O...O42 ^{iv}	0.89	0.89	0.89	1.88	1.83	1.85	2.765(6)	2.718(6)	2.739(7)	179.5	171.3	177.6
O99—H99P...O90	0.87	0.86	0.86	1.98	1.99	2.03	2.841(5)	2.849(4)	2.884(6)	171.2	171.5	171.0
Compound	4	5	6	4	5	6	4	5	6	4	5	6
O91—H91O...O21	0.84	0.84	0.84	1.94	1.93	1.95	2.771(4)	2.766(3)	2.779(3)	172.6	172.0	172.4
O91—H91P...O92	0.87	0.87	0.87	1.89	1.89	1.88	2.751(3)	2.749(3)	2.747(3)	171.4	169.5	171.6
O92—H92O...O93 ^v	0.79	0.80	0.79	2.20	2.18	2.19	2.927(3)	2.916(3)	2.918(3)	153.4	153.2	153.3
O92—H92P...O22 ^v	0.93	0.93	0.94	1.83	1.83	1.83	2.763(3)	2.764(3)	2.767(3)	174.5	174.4	174.6
O93—H93O...O21	0.84	0.84	0.85	1.88	1.88	1.88	2.716(3)	2.719(3)	2.719(3)	173.6	173.9	173.8
O93—H93P...O96	0.85	0.85	0.85	1.92	1.92	1.92	2.754(4)	2.750(3)	2.754(4)	164.3	163.4	164.5
O94—H94O...O22 ^{vi}	0.82	0.82	0.82	2.04	2.04	2.05	2.856(4)	2.855(3)	2.858(3)	170.2	170.2	170.6
O94—H94P...O93	0.91	0.91	0.92	1.82	1.82	1.82	2.722(4)	2.725(3)	2.726(4)	170.6	172.0	169.5
O95—H95O...O91	0.82	0.82	0.82	1.83	1.87	1.83	2.571(5)	2.601(4)	2.573(5)	149.3	148.2	149.5
O95—H95P...O97	0.81	0.81	0.80	1.80	1.84	1.80	2.569(5)	2.621(4)	2.568(5)	159.6	162.1	159.8
O96—H96O...O95	0.81	0.81	0.81	2.00	2.03	2.00	2.690(5)	2.720(4)	2.695(5)	143.0	142.7	143.2
O96—H96P...O94 ^{vii}	0.86	0.86	0.85	1.88	1.89	1.89	2.731(4)	2.744(3)	2.734(4)	173.2	173.0	172.4
O97—H97O...O22 ^{viii}	0.91	0.91	0.91	1.91	1.93	1.91	2.719(4)	2.724(3)	2.722(4)	147.8	144.8	147.6
O97—H97P...O95 ^{ix}	0.80	0.80	0.80	1.99	2.06	1.99	2.620(7)	2.708(5)	2.625(7)	134.6	137.4	135.1

Symmetry transformations used to generate equivalent atoms: (i) $-x+1, -y+1, -z+1$; (ii) $-x+1, -y+1, -z$; (iii) $-x+1, -y+2, -z$; (iv) $x, y-1, z$; (v) $-x+0.5, y+0.5, -z+0.5$; (vi) $-x+0.5, y-0.5, -z+0.5$; (vii) $-x+0.5, -y+1.5, -z+1$; (viii) $x, -y+2, z+0.5$; (ix) $-x+0.5, -y+2.5, -z+1$.

Table 4. Stacking and C-H... π interactions in the studied compounds [\AA , $^\circ$]. Each ring is indicated by one atom, which belongs solely to this ring. The α is a dihedral angle between planes I and J, β is an angle between Cg(I)-Cg(J) vector and normal to plane I, d_p is a perpendicular distance of Cg(I) on ring J plane.

R(I)...R(J)	d(Cg...Cg)			α			β			d_p		
Compound	1	2	3	1	2	3	1	2	3	1	2	3
R(N6)...R(C30) ⁱ	3.7641(2)	3.7862(1)	3.7505(4)	1	1	1	22.8	23.7	23.2	3.4512	3.4450	3.4462
Compound	4	5	6	4	5	6	4	5	6	4	5	6
R(C6)...R(C6) ⁱⁱ	3.7419(3)	3.8094(3)	3.7637(6)	0	0	0	27.0	28.0	27.0	3.3355	3.3643	3.3543
C-H...R(J)	d(H...Cg)			d(C...Cg)			$\angle(\text{CHCg})$					
Compound	1	2	3	1	2	3	1	2	3	1	2	3
C31—H31...R(N1) ⁱ	2.54	2.56	2.56	3.4887(2)	3.5117(1)	3.5087(4)	176.5	177.2	176.2			
C36—H36...R(N2)	2.98	2.97	3.04	3.7577(2)	3.7414(1)	3.7853(4)	140.1	139.6	136.3			
C42—H42B...R(C18) ⁱⁱⁱ	3.06	2.82	2.86	3.5908(2)	3.4092(1)	3.4196(4)	115.2	118.8	116.5			
C43—H43B...R(C30) ⁱ	3.24	3.04	2.99	4.2329(2)	3.8301(1)	3.7955(4)	172.7	136.8	138.9			
C44—H44A...R(N4) ⁱⁱⁱ	3.08	3.09	2.88	3.6046(2)	3.5341(1)	3.5678(4)	115.2	108.3	127.9			
C53—H53A...R(N1) ^{iv}	3.00	3.04	3.02	3.7713(2)	3.8131(1)	3.8256(4)	136.0	136.0	138.3			
C53—H53B...R(C6) ^{iv}	2.82	2.85	2.89	3.5052(2)	3.5133(1)	3.5353(4)	126.7	125.2	123.6			
C54—H54A...R(C18) ^v	2.88	2.85	3.03	3.7960(2)	3.7828(1)	3.8189(4)	156.4	159.2	138.2			
Compound	4	5	6	4	5	6	4	5	6	4	5	6
C22—H22...R(C18)	2.67	2.69	2.65	3.6608(3)	3.6823(3)	3.6455(6)	171.3	169.5	171.2			

Symmetry transformations used to generate equivalent atoms: (i) $-x, -y+2, -z$; (ii) $-x, -y+1, -z+1$; (iii) $x, y+1, z$; (iv) $-x+1, -y+1, -z+1$; (v) $x+1, y, z$.

Table 5. Vibrational frequencies and their assignments for the studied compounds.

Compound			Co(butyr) ₂	Ni(butyr) ₂	Cu(butyr) ₂	phen [23, 24, 53, 69]	Assignment
1	2	3					
3400 br	3400 br	3400 br					ν OH (H ₂ O)
3220 br	3220 br	3220 br					ν OH (H ₂ O)
3057 w	3057 w	3057 w				3058	ν CH (ar)
2958 m	2958 m	2958 w	2963 m	2963 m	2963 m		ν_{as} CH (CH ₃)
2928 w	2928 w	2928 w	2938 w	2935 w	2932 w		ν_{as} CH (CH ₂)
2870 w	2870 w	2870 w	2877 w	2975 w	2874 w		ν_s CH (CH ₃ , CH ₂)
1650 w	1650 w	1650 w					δ OH (H ₂ O)
1627 w	1627 w	1620 w				1617	ν CC (ar), ν CN (ar)
1552 s	1552 s	1563 s	1556 s	1557 s	1588 s		ν_{as} COO
1516 s	1516 s	1514 s				1506	ν CC (ar), ν CN (ar)
1496 w	1496 w	1495 w				1492	ρ CH (ar)
1462 w	1462 w	1455 w	1461 w	1460 w	1463 w		δ_{as} CH (CH ₃)
1425 s	1425 s	1425 s	1420 s	1419 s	1428 s		ν_s COO
1408 m	1408 m	1407 s				1405	ν CC (ar), ν CN (ar), δ CH (ar)
1349 m	1349 m	1347 m	1335 m	1340 m	1347 m	1345	δ_s CH (CH ₃), ν CC (ar), ν CN (ar), δ CH (ar)
1307 m	1307 m	1307 m	1315 m	1312 m	1317 m		τ CH (CH ₂)
1257 m	1257 m	1256 m	1246 m	1260 m	1265 m		ω CH (CH ₂)
1224 m	1224 m	1222 m	1212 w	1213 w	1213 w	1218	ω CH (CH ₂), τ CH (ar)
1147 m	1147 m	1144 m				1142	δ CH (ar)
1104 m	1104 m	1100 m	1101 w	1100 m	1105 m	1092	ν CCC (Pr), δ CH (ar)
1039 w	1039 w	1050 w	1048 w				ν CCC (Pr)
1005 w	1005 w	1005 w	1010 w				ν CCC (Pr)
970 w	970 w		930 m				ν CCC (Pr)
868 w	868 w	890 w	894 m	877 w	872 w	882	ν CCC (Pr), τ CH (ar)
848 s	848 s	851 s				855	τ CH (ar)
775 w	775 w	776 m	800 w	794 w	800 w	786	ω COO, ω CH (ar)
725 s	725 s	726 s	718 m	727 w	730 w	737	ρ CH (CH ₂), ω CH (ar)
642 w	642 w	644 w	644 w	667 w	655 m		σ COO
425 w	425 w	426 w	403 w	405 w	427 m		ν M–N

Compound			Co(ibutyr) ₂	Ni(ibutyr) ₂	Cu(ibutyr) ₂	phen [23, 24, 53, 69]	Assignment
4	5	6					
3400 br	3400 br	3400 br					ν OH (H ₂ O)
3210 br	3210 br	3210 br					ν OH (H ₂ O)
3054 w	3054 w	3054 w				3058	ν CH (ar)
2969 m	2969 m	2963 m	2969 m	2696 m	2966 m		ν_{as} CH (CH ₃)
2915 w	2915 w	2918 w	2934 w	2935 w	2933 w		ν CH (>CH-)
2875 w	2875 w	2867 w	2871 w	2871 w	2871 w		ν_s CH (CH ₃)
1654 w	1654 w						δ OH (H ₂ O)
1625 m	1625 m	1621 w				1617	ν CC (ar), ν CN (ar)
1551 s	1551 s	1560 s	1559 s	1568 s	1587 s		ν_{as} COO
1518 s	1518 s	1516 s				1506	ν CC (ar), ν CN (ar)
1495 w	1495 m	1495 w				1492	ρ CH (ar)
1472 m	1472 m	1469 m	1472 m	1472 m	1474 m		δ_{as} CH (CH ₃)
1425 s	1425 s	1425 s	1418 s	1420 s	1421 s		ν_s COO
1409 m	1409 m	1408 w				1405	ν CC (ar), ν CN (ar), δ CH (ar)
1366 m	1366 m	1366 m	1360 w	1360 w	1363 m		δ_s CH (CH ₃)
1346 w	1346 w					1345	ν CC (ar), ν CN (ar), δ CH (ar)
1307 m	1307 m	1309 w	1308 m		1315 m		δ CH (>CH-)
1284 m	1284 m	1273 m	1286 m	1290 m	1284 m		δ CH (>CH-)
1224 m	1224 m	1224 m				1218	τ CH (ar)
1206 w	1206 w	1210 w				1204	τ CH (ar)
1196 w	1196 w					1187	τ CH (ar)
1169 w	1169 w	1167 w	1169 w	1169 w	1169 w		δ CCC (iPr)
1148 m	1148 m	1142 m				1142	δ CH (ar)
1104 m	1104 m	1105 m	1099 s	1099 s	1097 s		δ CCC (iPr), δ CH (>CH-)
1088 m	1088 m	1090 m				1092	δ CH (ar)
970 w	970 w	960 w	964 w				δ CH (>CH-)
923 m	923 m	923 m	929 m	930 m	923 w		δ CH (>CH-)
868 w	868 w					882	τ CH (ar)
847 s	847 s	854 s	845 m	849 m	849 w	855	ν_s CCC (iPr), τ CH (ar)
775 w	775 w	783 m	762 w	779 w	784 w	786	ω COO, ω CH (ar)
727 s	727 s	727 s				737	ω CH (ar)
642 m	642 m	647 w	658 m	670 m	670 s		σ COO
531 w	531 w	531 w	560 w	572 w	565 w		δ CC (>CH-COO)
422 m	422 m	425 m	440 w	442 w	439 w		ν M–N

Vibrations symbols: w – weak, m – medium, s – strong, br – broadened, ν – stretching, δ – bending, ρ – rocking, σ – scissoring, τ – twisting, ω – wagging, s – symmetric, as – asymmetric, ar – aromatic ring, Pr – propyl group, iPr – isopropyl group.

Table 6. Absorption maxima (nm) and their assignment for the studied compounds.

Compound		Assignment	Compound		Assignment	Compound		Assignment
1	4		2	5		3	6	
218	221	$\pi \rightarrow \pi^*$ (phen)	218	220	$\pi \rightarrow \pi^*$ (phen)	218	218	$\pi \rightarrow \pi^*$ (phen)
254	261	$\pi \rightarrow \pi^*$ (phen)	254	260	$\pi \rightarrow \pi^*$ (phen)	254	256	$\pi \rightarrow \pi^*$ (phen)
294	295	$n \rightarrow \pi^*$ (phen)	294	295	$n \rightarrow \pi^*$ (phen)	294	294	$n \rightarrow \pi^*$ (phen)
325	325	$n \rightarrow \pi^*$ (phen)	326	327	$n \rightarrow \pi^*$ (phen)	330	326	$n \rightarrow \pi^*$ (phen)
350	348	$n \rightarrow \pi^*$ (phen)	340	341	$n \rightarrow \pi^*$ (phen)	348	346	$n \rightarrow \pi^*$ (phen)
446	442	LMCT	410	411	LMCT			
540	534	${}^4T_{1g}(F) \rightarrow {}^4T_{1g}(P)$	520	534	${}^3A_{2g} \rightarrow {}^3T_{1g}(P)$	682	678	${}^2B_{1g} \rightarrow {}^2E_g, {}^2B_{1g} \rightarrow {}^2B_{2g}, {}^2B_{1g} \rightarrow {}^2A_{1g}$
			785	784	${}^3A_{2g} \rightarrow {}^3T_{1g}(F)$			

Table 7. Temperature ranges, mass losses / residual mass (experimental/theoretical) and removal species / final products of thermal decomposition steps of the studied compounds.

Compound					
1	2	3	4	5	6
40 °C – 185 °C	40 °C – 185 °C	40 °C – 175 °C	30 °C – 175 °C	30 °C – 130 °C	40 °C – 170 °C
16.14% / 16.68%	16.56% / 15.40%	16.67% / 16.60%	21.04% / 21.07%	21.11% / 21.07%	21.19% / 20.98%
- 9 H ₂ O	- 8.18 H ₂ O	- 9 H ₂ O	- 12 H ₂ O	- 12 H ₂ O	- 12 H ₂ O
185 °C – 360 °C	a) 185 °C – 360 °C	a) 175 °C – 400 °C	175 °C – 370 °C	a) 175 °C – 360 °C	170 °C – 340 °C
19.79% / 19.98%	14.42% / -	26.52% / -	19.13% / 18.95%	16.38% / -	19.97% / 18.85%
- 2 H ₂ O, -2 butyr, + 0.5 O ₂	b) 360 °C – 500 °C	b) 400 °C – 520 °C	- 2 H ₂ O, -2 ibutyr, + 0.5 O ₂	b) 360 °C – 490 °C	- 2 H ₂ O, -2 ibutyr, + 0.5 O ₂
	60.77% / -	50.77% / -		55.76% / -	
370 °C – 500 °C	Totally	Totally	370 °C – 490 °C	Totally	340 °C – 550 °C
55.25% / 55.63%	75.19% / 76.79%	76.29% / 75.25%	52.17% / 52.69%	72.14% / 71.64%	50.78% / 52.46%
- 3 phen	- 2 H ₂ O, -2 butyr, -3 phen, + 0.5 O ₂	- 2 H ₂ O, -2 butyr, -3 phen, + 0.5 O ₂	- 3 phen	- 2 H ₂ O, -2 ibutyr, -3 phen, + 0.5 O ₂	- 3 phen
500 °C	500 °C	520 °C	490 °C	490 °C	550 °C
8.82% / 7.71%	8.25% / 7.81%	7.04% / 8.15%	7.66% / 7.29%	6.75% / 7.29%	8.06% / 7.71%
CoO	NiO	CuO	CoO	NiO	CuO

References

- [1] A. Trzesowska-Kruszynska, J. Mol. Struct. 1072 (2014) 284.
- [2] R. Kruszynski, T. Sieranski, M. Swiatkowski, M. Zielak, J. Wojciechowski, M. Dzierawska, E. Czubacka, J. Chem. Crystallogr. 45 (2015) 484.
- [3] J. Mitra, K. Pal, S. Sarkar, Dalton Trans. 42 (2013) 13905.
- [4] A. Trzesowska-Kruszynska, J. Coord. Chem. 64 (2011) 663-678.
- [5] L. Radovanovic, J. Rogan, D. Poleti, M. Milutinovic, M. Rodic, Polyhedron 112 (2016) 18.
- [6] J. D. Einkauf, B. C. Chan, D. T. de Lill, Polyhedron 128 (2017) 149.
- [7] B. Nowicka, W. Nitek, P. Pietrzyk, B. Sieklucka, Polyhedron 119 (2016) 1.
- [8] A. Trzesowska-Kruszynska, J. Coord. Chem. 67 (2014) 120-135.
- [9] D. Czakis-Sulikowska, J. Kaluzna, J. Therm. Anal. 47 (1996) 1763.
- [10] D. Czakis-Sulikowska, J. Kaluzna, J. Radwanska-Doczekalska, J. Therm. Anal. Calorim. 54 (1998) 103.
- [11] D. Czakis-Sulikowska, J. Kaluzna, J. Therm. Anal. Calorim. 58 (1999) 51.
- [12] D. Czakis-Sulikowska, J. Kaluzna-Czaplinska, J. Therm. Anal. Calorim. 62 (2000) 821.
- [13] G.E. Jackson, A.N. Hammouda, F.M. Elmagbari, R.P. Bono, Polyhedron 123 (2017) 23.
- [14] R.A. Agarwal, N.K. Gupta, Coord. Chem. Rev. 332 (2017) 100.
- [15] M. Azam, S.I. Al-Resayes, A. Trzesowska-Kruszynska, R. Kruszynski, P. Kumar, S.L. Jain, Polyhedron 124 (2017) 177.
- [16] J.G. Malecki, R. Kruszynski, Z. Mazurak, Polyhedron 28 (2009) 3891.
- [17] R. Kruszynski, A. Malinowska, D. Czakis-Sulikowska, A. Lamparska, J. Coord. Chem. 62 (2009) 911.
- [18] J.G. Malecki, M. Jaworska, R. Kruszynski, J. Organomet. Chem. 693 (2007) 2903.
- [19] J.H.N. Buttery, Effendy, S. Mutofin, N.C. Plackett, B.W. Skelton, N. Somers, C.R. Whitaker, A.H. White, Z. Anorg. Allg. Chem. 632 (2006) 1839.
- [20] C.R. Groom, I.J. Bruno, M.P. Lightfoot, S.C. Ward, Acta Crystallogr. B 72 (2016) 171.
- [21] B.W. Skelton, A.F. Waters, A.H. White, Aust. J. Chem. 49 (1996) 99.
- [22] D.W. Margerum, C.V. Banks, Anal. Chem. 26 (1954) 200.
- [23] T. Sieranski, R. Kruszynski, J. Therm. Anal. Calorim. 109 (2012) 141.
- [24] R. Kruszynski, Inorg. Chim. Acta 371 (2011) 111.
- [25] P. Szymanski, T. Fraczek, M. Markowicz, E. Mikiciuk-Olasik, Biometals 25 (2012) 1089.
- [26] M. Barcelo-Olivier, A. Garcia-Raso, A. Terron, E. Molins, M.J. Prieto, V. Moreno, J. Martinez, V. Llado, I. Lopez, A. Gutierrez, P.V. Escriba, J. Inorg. Biochem. 101 (2007) 649.
- [27] H. Mansouri-Torshizi, M. Saeidifar, Z.Y. Ghasemi, M. Khashtan, A. Divsalar, A.A. Saboury, J. Korean Chem. Soc., 55 (2011) 70.
- [28] Y. Geldmacher, I. Kitano, H. Alborzina, K. Bergerhoff, R. Rubbiani, P. Wefelmeier, A. Prokop, R. Gust, I. Ott, S. Wölfl, W.S. Sheldrick, ChemMedChem 6 (2011) 429.

- [29] S. Chandraleka, K. Ramya, G. Chandramohan, D. Dhanasekaran, A. Priyadharshini, A. Panneerselvam, J. Saudi Chem. Soc. 18 (2014) 953.
- [30] A. Aliakbari, E. Najafi, M.M. Amini, S.W. Ng, Monatsh. Chem. 145 (2014) 1277.
- [31] A. Barakat, M. Al-Noaimi, M. Suleiman, A.S. Aldwayyan, B. Hammouti, T.B. Hadda, S.F. Haddad, A. Boshala, I. Warad, Int. J. Mol. Sci. 14 (2013) 23941.
- [32] N. Srinivasan, S. Thirumaran, S. Ciattini, J. Mol. Struct. 1026 (2012) 102.
- [33] F.J. Welcher, *Analityczne zastosowanie kwasu wersenowego* (eng. The Analytical Uses of Etylenediamineteraacetic Acid), WNT, Warsaw, Poland, 1963.
- [34] X-RED. Version 1.18. STOE & Cie GmbH, Darmstadt, Germany, 1999.
- [35] G.M. Sheldrick, Acta Crystallogr. A 71 (2015) 3.
- [36] G.M. Sheldrick, Acta Crystallogr. C 71 (2015) 3.
- [37] G.M. Sheldrick, Acta Crystallogr. A 64 (2008) 112.
- [38] Powder Diffraction File International Center of Diffraction Data, 12 Campus Boulevard, Newton Square, PA, USA, 2003.
- [39] W. Mizerski, *Tablice chemiczne* (eng. Chemical Tables), Wydawnictwo Adamantan, Warsaw, Poland, 2004.
- [40] D.L. Kepert, in: S.J. Lippard (Ed.), *Progress in Inorganic Chemistry*, John Wiley & Sons, Inc., Hoboken, NJ, USA, 1997, pp. 1-65.
- [41] W.H. Zachariasen, J. Less-Common Met. 62 (1978) 1.
- [42] I.D. Brown, Acta Crystallogr. B 53 (1997) 381.
- [43] I.D. Brown, Acta Crystallogr. B 48 (1992) 553.
- [44] M. O'Keeffe, N.E. Brese, Acta Crystallogr. B 47 (1997) 192.
- [45] A. Trzesowska, R. Kruszynski, T.J. Bartczak, Acta Crystallogr. B 60 (2004) 174.
- [46] A. Trzesowska, R. Kruszynski, T.J. Bartczak, Acta Crystallogr. B 61 (2005) 429.
- [47] A. Trzesowska, R. Kruszynski, T.J. Bartczak, Acta Crystallogr. B 62 (2006) 745.
- [48] G.J. Palenik, Inorg. Chem. 42 (2003) 2725.
- [49] T.A. Mimaya, A.P. Polishchuk, A.S. Tolochko, S.V. Volkov, Kristallografiya, 38 (1993) 49.
- [50] N. Aurangzeb, C.E. Hulme, C.A. McAuliffe, R.G. Pritchard, M. Watkinson, M.R. Bermejo, A. Sousa, Chem. Commun. (1994) 2193.
- [51] C. Schaffer, H. Bogge, A. Merca, I.A. Weinstock, D. Rehder, E.T.K. Haupt, A. Muller, Angew. Chem. Int. Edit. 48 (2009) 8051.
- [52] L. Infantes, J. Chisholm, S. Motherwell, CrystEngComm 5 (2003) 480.
- [53] M. Swiatkowski, R. Kruszynski, J. Coord. Chem. 70 (2017) 642.
- [54] E.G. Il'na, S.I. Troyanov, K.M. Dunaeva, Russ. J. Coord. Chem. 18 (1992) 882.
- [55] G.B. Deacon, R.J. Phillips, Coord. Chem. Rev. 33 (1980) 227.
- [56] K. Nakamoto, *Infrared and Raman Spectra of Inorganic and Coordination Compounds*, John Wiley and Sons, New York, USA, 1997.
- [57] Y. Deng, Y. Bai, L.-G. Zhu, J.-X. Jiang, G.-Q. Lai, J. Coord. Chem. 65 (2012) 2793.
- [58] A. Prisecaru, V. McKee, O. Howe, G. Rochford, M. McCann, J. Collieran, M. Pour, N. Barron, N. Gathergood, A. Kellett, J. Med. Chem. 56 (2013) 8599.
- [59] A.B.P. Lever, *Inorganic Electronic Spectroscopy*, second ed., Elsevier, Amsterdam, 1984.
- [60] J. Rogan, D. Poleti, L. Karanovic, G. Bogdanovic, A. Spasojevic-de Bire, D.M. Petrovic, Polyhedron 19 (2000) 1415.
- [61] E. Vinuelas-Zahinos, M.A. Maldonado-Rogado, F. Luna-Giles, F.J. Barros-Garcia, Polyhedron 27 (2008) 879.
- [62] L.S. Skorokhod, I.I. Seifullina, V.V. Minin, V.G. Vlasenko, I.V. Pirog, Russ. J. Inorg. Chem. 52 (2007) 1006.
- [63] B.K. Das, S.J. Bora, M. Chakraborty, L. Kalita, R. Chakrabarty, R. Barman, J. Chem. Sci. 118 (2006) 487.
- [64] G.G. Mohamed, Spectrochim. Acta A 62 (2005) 1165.
- [65] G.Y. Nagesh, K.M. Raj, B.H.M. Mruthyunjayaswamy, J. Mol. Struct. 1079 (2015) 423.
- [66] R.P. Sharma, S. Kumar, A. Saini, P. Venugopalan, A. Rodriguez-Dieguez, J.M. Salas, J. Mol. Struct. 1071 (2014) 11.
- [67] J.M. Seco, M.J. Gonzalez Garmendia, M. Quiros, J. Coord. Chem. 55 (2002) 345.
- [68] S. Kumar, R.P. Sharma, P. Venugopalan, J. Jezierska, A. Wojciechowska, V. Ferretti, Inorg. Chim. Acta 432 (2015) 221.
- [69] M.J. Muniz-Miranda, J. Phys. Chem. A 104 (2000) 7803.

Figure 1

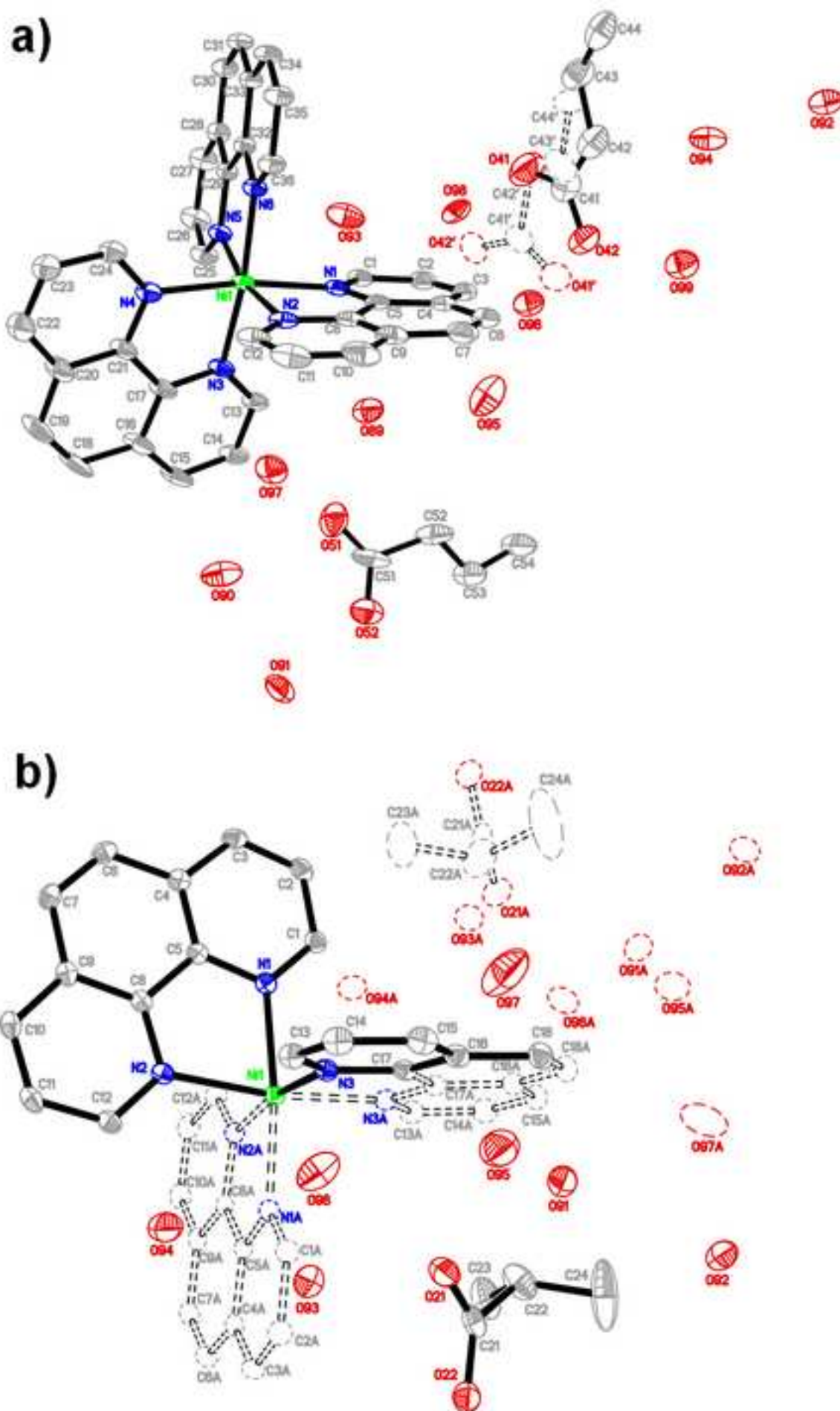


Figure 2

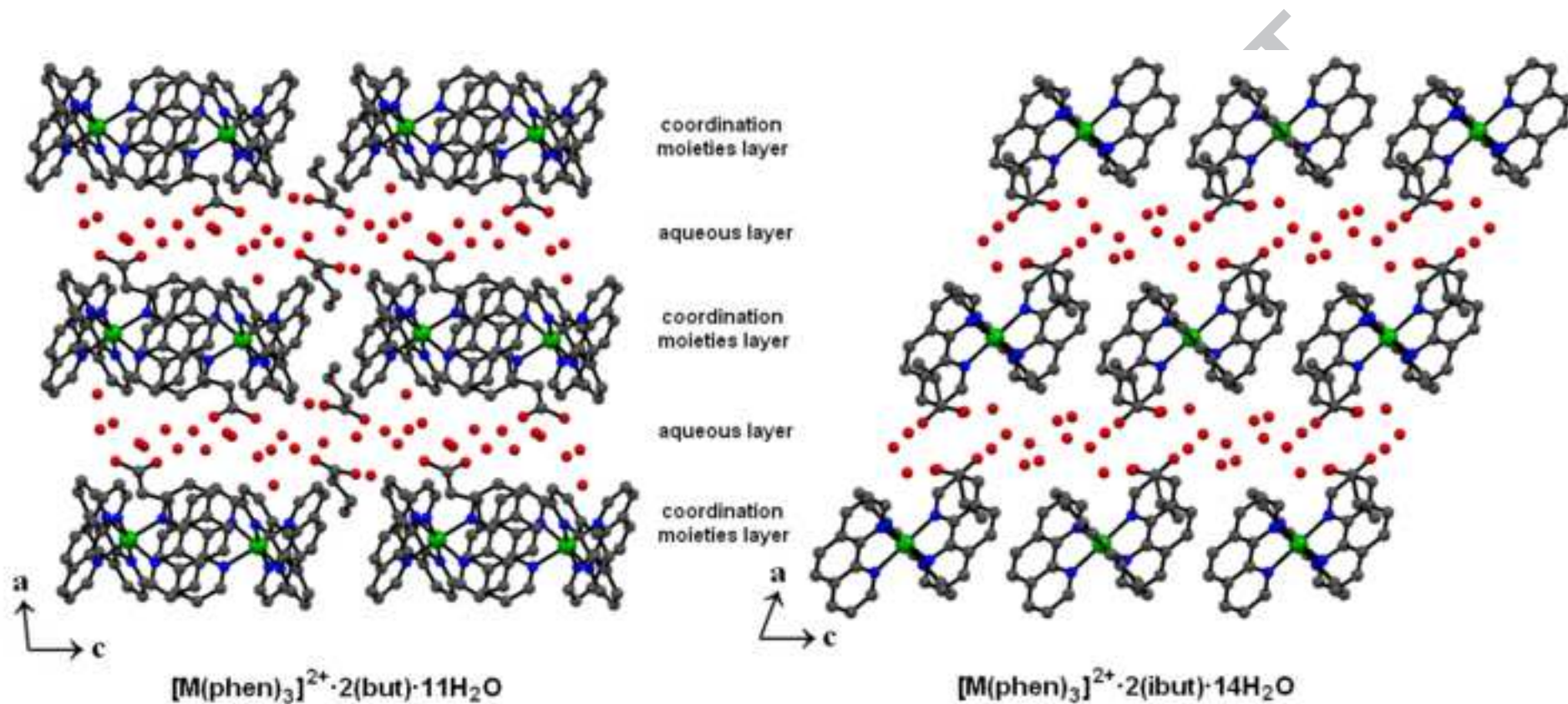


Figure 3

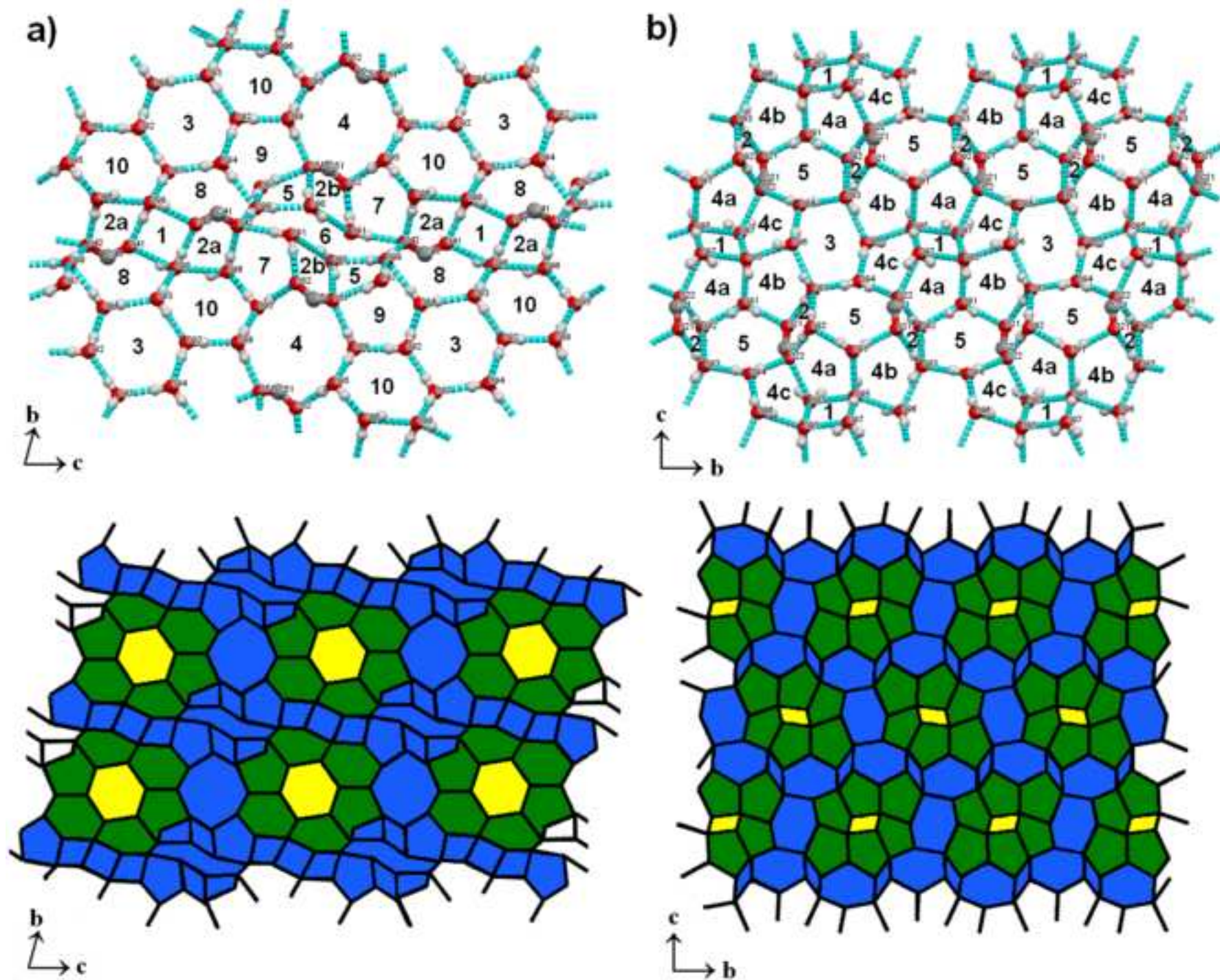


Figure 4

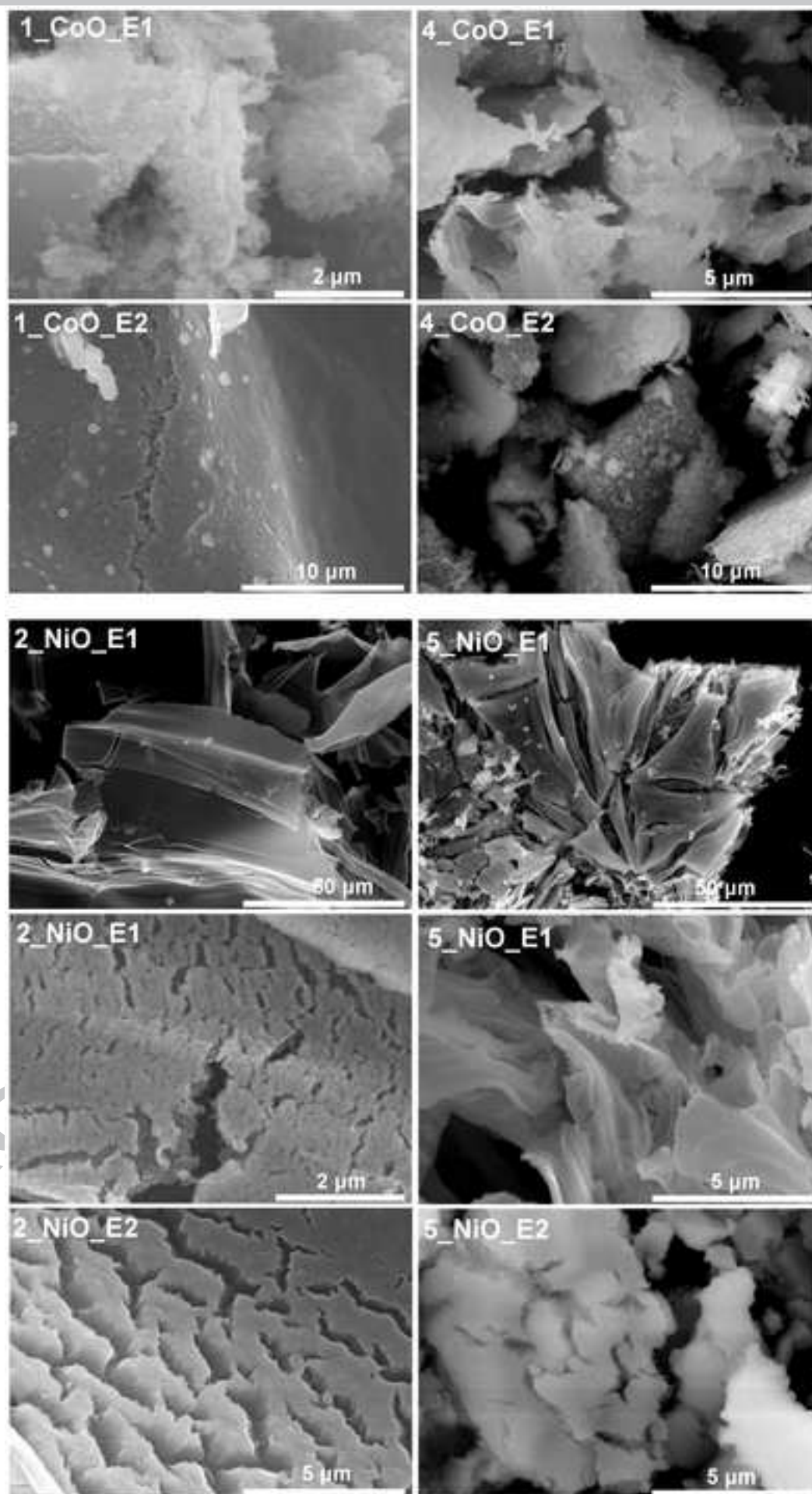
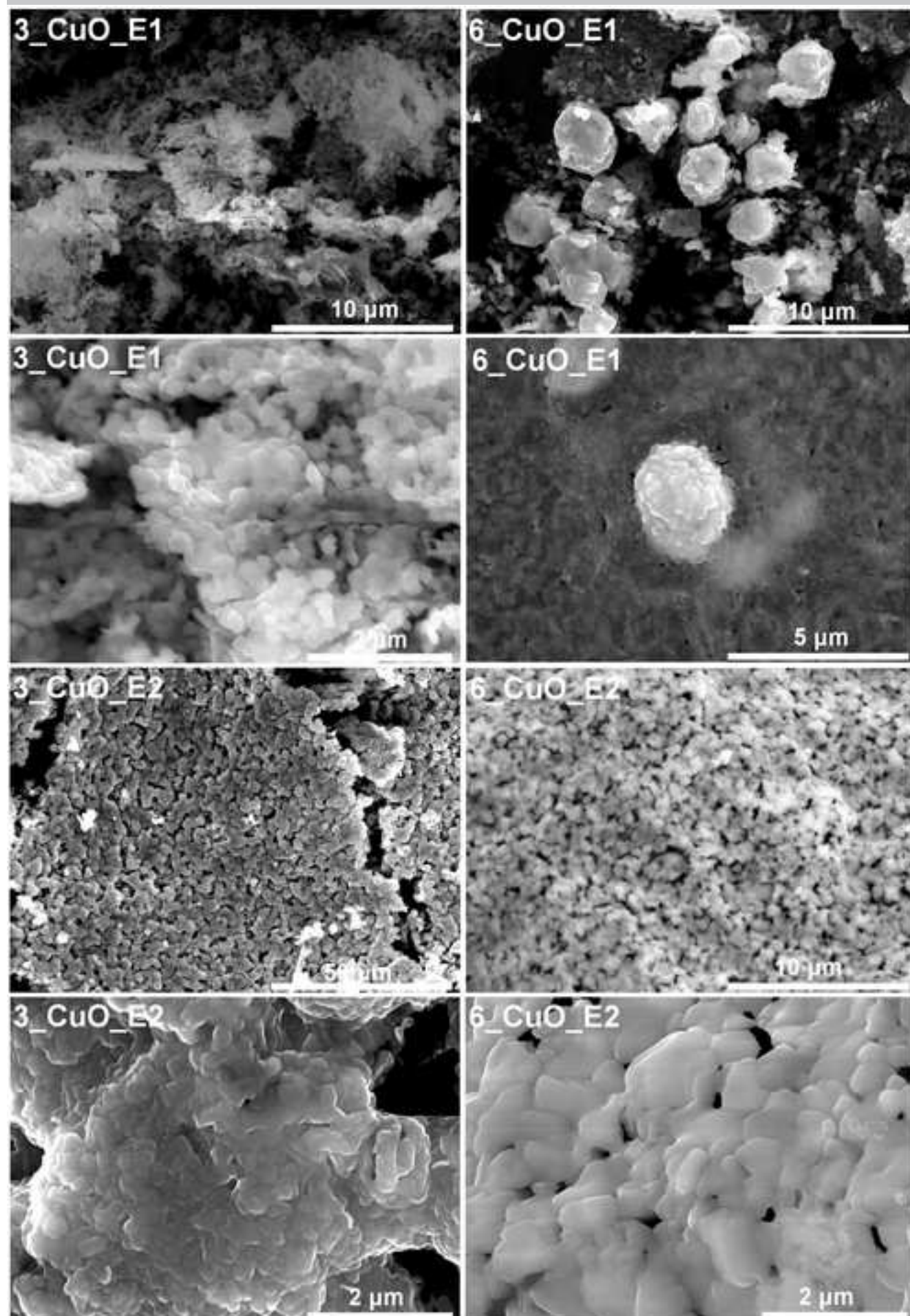
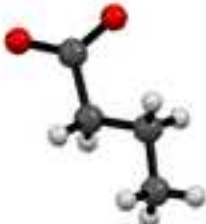



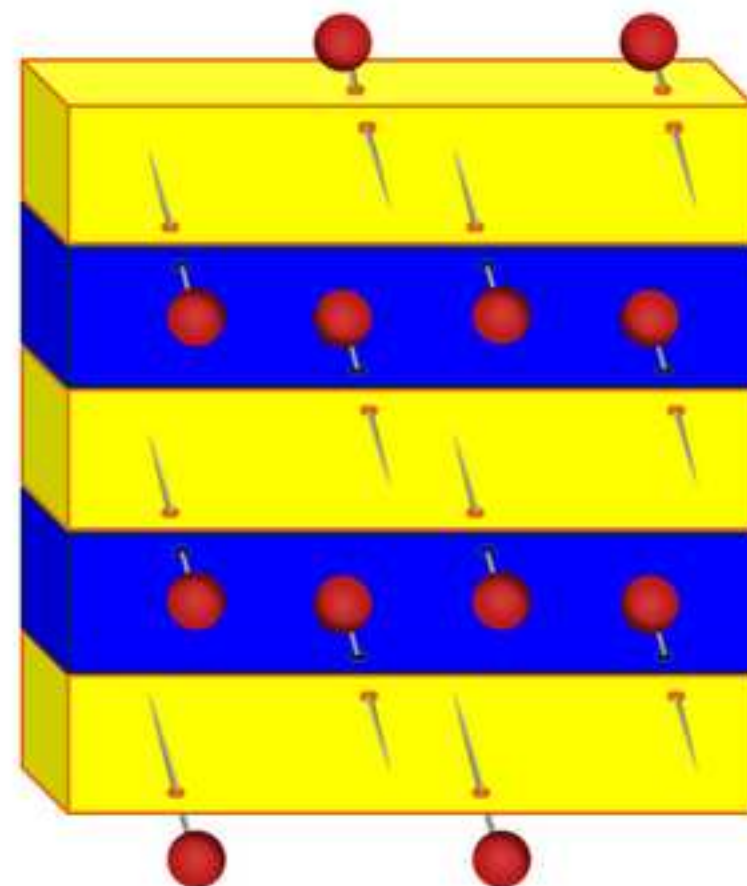
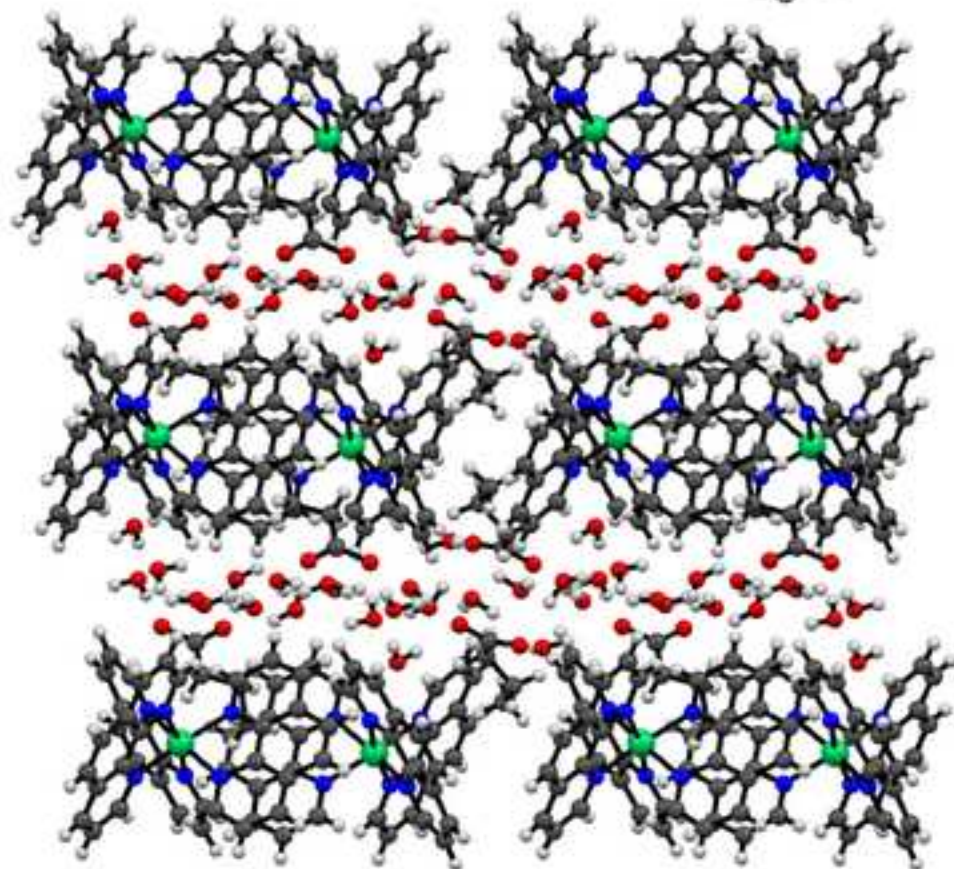
Figure 5

ACCEPTED MANUSCRIPT



Structural insights into the usage of

carboxylate ions  as  molecular pins



Synopsis

The two series of new isostructural coordination compounds containing cobalt, nickel, copper butyrates or isobutyrate and 1,10-phenanthroline were synthesized, structurally characterized, and their spectroscopic and thermal properties were investigated. The studied compounds exhibit layered packing in crystal net. The carboxylate anions function as linkers between these layers and allow pinning them together *via* hydrogen bonds and C—H... π intermolecular interactions. Due to placement of carboxylate anions out of coordination moieties, the presented compounds can be ideal standards in spectroscopic determinations of coordination type of but and ibut ions in coordination compounds.